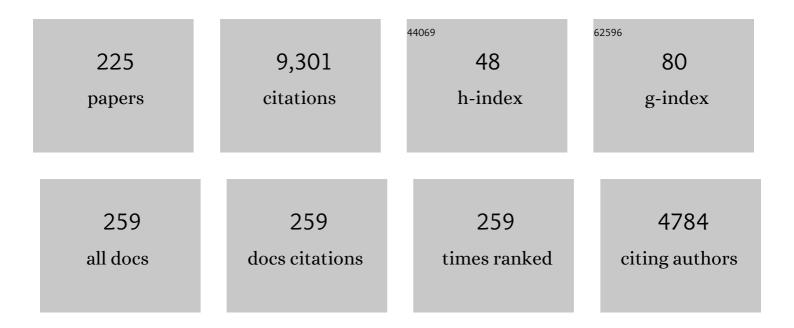
List of Publications by Year in descending order

Source: https://exaly.com/author-pdf/8589744/publications.pdf

Version: 2024-02-01



#	Article	IF	CITATIONS
1	LevelÂ2 processor and auxiliary data for ESA Version 8 final full mission analysis of MIPAS measurements on ENVISAT. Atmospheric Measurement Techniques, 2022, 15, 1871-1901.	3.1	2
2	CO2 retrievals in the Mars daylight thermosphere from its 4.3â€î¼m limb emission measured by OMEGA/MEx. Icarus, 2021, 353, 113830.	2.5	6
3	Modelling the He I triplet absorption at 10 830 â"« in the atmospheres of HD 189733 b and GJ 3470 b. Astronomy and Astrophysics, 2021, 647, A129.	5.1	27
4	Evidence of energy-, recombination-, and photon-limited escape regimes in giant planet H/He atmospheres. Astronomy and Astrophysics, 2021, 648, L7.	5.1	19
5	IMK/IAA MIPAS temperature retrieval version 8: nominal measurements. Atmospheric Measurement Techniques, 2021, 14, 4111-4138.	3.1	13
6	Spectroscopy, gas kinetics, and opacity of thermospheric nitric oxide and implications for analysis of SABER infrared emission measurements at 5.3 Âμm. Journal of Quantitative Spectroscopy and Radiative Transfer, 2021, 268, 107609.	2.3	7
7	The ESA MIPAS/Envisat level2-v8 dataset: 10 years of measurements retrieved with ORM v8.22. Atmospheric Measurement Techniques, 2021, 14, 7975-7998.	3.1	5
8	Improving the Understanding of CrIS Full Spectral Resolution Nonlocal Thermodynamic Equilibrium Radiances Using Spectral Correlation. Journal of Geophysical Research D: Atmospheres, 2020, 125, e2020JD032710.	3.3	4
9	First Detection of a Brief Mesoscale Elevated Stratopause in Very Early Winter. Geophysical Research Letters, 2020, 47, e2019GL086751.	4.0	4
10	Modelling the Heâ€ī triplet absorption at 10 830 â,,« in the atmosphere of HD 209458 b. Astronomy and Astrophysics, 2020, 636, A13.	5.1	49
11	Discriminating between hazy and clear hot-Jupiter atmospheres with CARMENES. Astronomy and Astrophysics, 2020, 643, A24.	5.1	13
12	Distinguishing between Wet and Dry Atmospheres of TRAPPIST-1 e and f. Astrophysical Journal, 2020, 901, 126.	4.5	33
13	Climatology of CH4, HCN and C2H2 in Titan's upper atmosphere from Cassini/VIMS observations. Icarus, 2019, 331, 83-97.	2.5	5
14	No detection of methane on Mars from early ExoMars Trace Gas Orbiter observations. Nature, 2019, 568, 517-520.	27.8	111
15	Martian dust storm impact on atmospheric H2O and D/H observed by ExoMars Trace Gas Orbiter. Nature, 2019, 568, 521-525.	27.8	107
16	Multiple water band detections in the CARMENES near-infrared transmission spectrum of HD 189733 b. Astronomy and Astrophysics, 2019, 621, A74.	5.1	57
17	Methane on Mars: New insights into the sensitivity of CH4 with the NOMAD/ExoMars spectrometer through its first in-flight calibration. Icarus, 2019, 321, 671-690.	2.5	32
18	The CARMENES search for exoplanets around M dwarfs. Astronomy and Astrophysics, 2018, 609, A117.	5.1	103

#	Article	IF	CITATIONS
19	Detection of Heâ€TI λ10830 â",« absorption on HD 189733 b with CARMENES high-resolution transmission spectroscopy. Astronomy and Astrophysics, 2018, 620, A97.	5.1	120
20	The CARMENES search for exoplanets around M dwarfs. Astronomy and Astrophysics, 2018, 609, L5.	5.1	46
21	Ground-based detection of an extended helium atmosphere in the Saturn-mass exoplanet WASP-69b. Science, 2018, 362, 1388-1391.	12.6	174
22	The CARMENES search for exoplanets around M dwarfs. Astronomy and Astrophysics, 2018, 612, A49.	5.1	173
23	Aerosols and Water Ice in Jupiter's Stratosphere from UV-NIR Ground-based Observations. Astronomical Journal, 2018, 156, 169.	4.7	7
24	On the improved stability of the version 7 MIPAS ozone record. Atmospheric Measurement Techniques, 2018, 11, 4693-4705.	3.1	7
25	NOMAD, an Integrated Suite of Three Spectrometers for the ExoMars Trace Gas Mission: Technical Description, Science Objectives and Expected Performance. Space Science Reviews, 2018, 214, 1.	8.1	95
26	On Longâ€Term SABER CO ₂ Trends and Effects Due to Nonuniform Space and Time Sampling. Journal of Geophysical Research: Space Physics, 2018, 123, 7958-7967.	2.4	20
27	Modeling of Nonlocal Thermodynamic Equilibrium Effects in the Classical and Principal Componentâ€Based Version of the RTTOV Fast Radiative Transfer Model. Journal of Geophysical Research D: Atmospheres, 2018, 123, 5741-5761.	3.3	8
28	MIPAS observations of ozone in the middle atmosphere. Atmospheric Measurement Techniques, 2018, 11, 2187-2212.	3.1	11
29	Spatial and Temporal Structure of the Tertiary Ozone Maximum in the Polar Winter Mesosphere. Journal of Geophysical Research D: Atmospheres, 2018, 123, 4373-4389.	3.3	8
30	CARMENES: high-resolution spectra and precise radial velocities in the red and infrared. , 2018, , .		37
31	Semidiurnal tidal activity of the middle atmosphere at mid-latitudes derived from O2 atmospheric and OH(6-2) airglow SATI observations. Journal of Atmospheric and Solar-Terrestrial Physics, 2017, 164, 116-126.	1.6	5
32	Validation of the MIPAS CO ₂ volume mixing ratio in the mesosphere and lower thermosphere and comparison with WACCM simulations. Journal of Geophysical Research D: Atmospheres, 2017, 122, 8345-8366.	3.3	14
33	ALMA Discovery of Dust Belts around Proxima Centauri. Astrophysical Journal Letters, 2017, 850, L6.	8.3	59
34	CO concentration in the upper stratosphere and mesosphere of Titan from VIMS dayside limb observations at 4.7 Âμm. Icarus, 2017, 293, 119-131.	2.5	5
35	HEPPA-II model–measurement intercomparison project: EPP indirect effects during the dynamically perturbed NH winter 2008–2009. Atmospheric Chemistry and Physics, 2017, 17, 3573-3604.	4.9	55
36	Mesospheric OH layer altitude at midlatitudes: variability over the Sierra Nevada Observatory in Granada, Spain (37°†N, 3°†W). Annales Geophysicae, 2017, 35, 1151-1164.	1.6	10

#	Article	IF	CITATIONS
37	Energetic particle precipitation: A major driver of the ozone budget in the Antarctic upper stratosphere. Geophysical Research Letters, 2016, 43, 3554-3562.	4.0	42
38	Optical and radiometric models of the NOMAD instrument part II: the infrared channels - SO and LNO. Optics Express, 2016, 24, 3790.	3.4	25
39	CARMENES: an overview six months after first light. Proceedings of SPIE, 2016, , .	0.8	59
40	On the secular trend of CO x and CO 2 in the lower thermosphere. Journal of Geophysical Research D: Atmospheres, 2016, 121, 3634-3644.	3.3	20
41	MIPAS observations of longitudinal oscillations in the mesosphere and the lower thermosphere: climatology of odd-parity daily frequency modes. Atmospheric Chemistry and Physics, 2016, 16, 11019-11041.	4.9	6
42	Measurements of global distributions of polar mesospheric clouds during 2005–2012 by MIPAS/Envisat. Atmospheric Chemistry and Physics, 2016, 16, 6701-6719.	4.9	10
43	A semi-empirical model for mesospheric and stratospheric NO _{<i>y</i>} produced by energetic particle precipitation. Atmospheric Chemistry and Physics, 2016, 16, 8667-8693.	4.9	20
44	Expected performances of the NOMAD/ExoMars instrument. Planetary and Space Science, 2016, 124, 94-104.	1.7	31
45	Titan Science with the <i>James Webb Space Telescope</i> . Publications of the Astronomical Society of the Pacific, 2016, 128, 018007.	3.1	19
46	Global distributions of CO ₂ volume mixing ratio in the middle and upper atmosphere from daytime MIPAS high-resolution spectra. Atmospheric Measurement Techniques, 2016, 9, 6081-6100.	3.1	9
47	Optical and radiometric models of the NOMAD instrument part I: the UVIS channel. Optics Express, 2015, 23, 30028.	3.4	26
48	The heating efficiency of the exothermic reaction HÂ+ÂO ₃ in the mesosphere. Journal of Geophysical Research D: Atmospheres, 2015, 120, 12739-12747.	3.3	5
49	Vibrationalâ€vibrational and vibrationalâ€thermal energy transfers of CO 2 with N 2 from MIPAS highâ€resolution limb spectra. Journal of Geophysical Research D: Atmospheres, 2015, 120, 8002-8022.	3.3	10
50	Increasing carbon dioxide concentration in the upper atmosphere observed by SABER. Geophysical Research Letters, 2015, 42, 7194-7199.	4.0	41
51	The EChO science case. Experimental Astronomy, 2015, 40, 329-391.	3.7	31
52	The NIR transmission spectrum of Jupiter from the observation of a Ganymede's eclipse. EPJ Web of Conferences, 2015, 101, 06048.	0.3	0
53	Comparison of nitric oxide measurements in the mesosphere and lower thermosphere from ACE-FTS, MIPAS, SCIAMACHY, and SMR. Atmospheric Measurement Techniques, 2015, 8, 4171-4195.	3.1	17
54	JUPITER AS AN EXOPLANET: UV TO NIR TRANSMISSION SPECTRUM REVEALS HAZES, A Na LAYER, AND POSSIBLY STRATOSPHERIC H ₂ O-ICE CLOUDS. Astrophysical Journal Letters, 2015, 801, L8.	8.3	33

#	Article	IF	CITATIONS
55	Rotational temperatures of Venus upper atmosphere as measured by SOIR on board Venus Express. Planetary and Space Science, 2015, 113-114, 347-358.	1.7	38
56	Science objectives and performances of NOMAD, a spectrometer suite for the ExoMars TGO mission. Planetary and Space Science, 2015, 119, 233-249.	1.7	77
57	Mesospheric and stratospheric NO _{<i>y</i>} produced by energetic particle precipitation during 2002–2012. Journal of Geophysical Research D: Atmospheres, 2014, 119, 4429-4446.	3.3	75
58	Changes in the composition of the northern polar upper stratosphere in February 2009 after a sudden stratospheric warming. Journal of Geophysical Research D: Atmospheres, 2014, 119, 11,429.	3.3	9
59	MIPAS temperature from the stratosphere to the lower thermosphere: Comparison of vM21 with ACE-FTS, MLS, OSIRIS, SABER, SOFIE and lidar measurements. Atmospheric Measurement Techniques, 2014, 7, 3633-3651.	3.1	30
60	Nighttime ozone variability in the high latitude winter mesosphere. Journal of Geophysical Research D: Atmospheres, 2014, 119, 13,547.	3.3	14
61	Hemispheric distributions and interannual variability of NO _{<i>y</i>} produced by energetic particle precipitation in 2002–2012. Journal of Geophysical Research D: Atmospheres, 2014, 119, 13,565.	3.3	39
62	On the distribution of CO ₂ and CO in the mesosphere and lower thermosphere. Journal of Geophysical Research D: Atmospheres, 2014, 119, 5700-5718.	3.3	90
63	Middle atmospheric changes caused by the January and March 2012 solar proton events. Atmospheric Chemistry and Physics, 2014, 14, 1025-1038.	4.9	40
64	Variability of NO _x in the polar middle atmosphere from October 2003 to March 2004: vertical transport vs. local production by energetic particles. Atmospheric Chemistry and Physics, 2014, 14, 7681-7692.	4.9	18
65	An unidentified emission in Titan's upper atmosphere. Geophysical Research Letters, 2013, 40, 1489-1493.	4.0	44
66	Satellite observations of ozone in the upper mesosphere. Journal of Geophysical Research D: Atmospheres, 2013, 118, 5803-5821.	3.3	63
67	LARGE ABUNDANCES OF POLYCYCLIC AROMATIC HYDROCARBONS IN TITAN'S UPPER ATMOSPHERE. Astrophysical Journal, 2013, 770, 132.	4.5	106
68	An observational and theoretical study of the longitudinal variation in neutral temperature induced by aurora heating in the lower thermosphere. Journal of Geophysical Research: Space Physics, 2013, 118, 7410-7425.	2.4	32
69	The solar proton events in 2012 as observed by MIPAS. Geophysical Research Letters, 2013, 40, 2339-2343.	4.0	41
70	Ten years of MIPAS measurements with ESA Level 2 processor V6 – Part 1: Retrieval algorithm and diagnostics of the products. Atmospheric Measurement Techniques, 2013, 6, 2419-2439.	3.1	66
71	Retrieval of nitric oxide in the mesosphere and lower thermosphere from SCIAMACHY limb spectra. Atmospheric Measurement Techniques, 2013, 6, 2521-2531.	3.1	17
72	Radiative and energetic constraints on the global annual mean atomic oxygen concentration in the mesopause region. Journal of Geophysical Research D: Atmospheres, 2013, 118, 5796-5802.	3.3	26

#	Article	IF	CITATIONS
73	The global picture of the atmospheric composition provided by MIPAS on Envisat. , 2012, , .		3
74	Observed temporal evolution of global mean age of stratospheric air for the 2002 to 2010 period. Atmospheric Chemistry and Physics, 2012, 12, 3311-3331.	4.9	181
75	Impact of January 2005 solar proton events on chlorine species. Atmospheric Chemistry and Physics, 2012, 12, 4159-4179.	4.9	19
76	On the quality of MIPAS kinetic temperature in the middle atmosphere. Atmospheric Chemistry and Physics, 2012, 12, 6009-6039.	4.9	30
77	EChO. Experimental Astronomy, 2012, 34, 311-353.	3.7	98
78	GRANADA: A Generic RAdiative traNsfer AnD non-LTE population algorithm. Journal of Quantitative Spectroscopy and Radiative Transfer, 2012, 113, 1771-1817.	2.3	60
79	Global observations of thermospheric temperature and nitric oxide from MIPAS spectra at 5.3 <i>μ</i> m. Journal of Geophysical Research, 2011, 116, n/a-n/a.	3.3	46
80	Northern Hemisphere atmospheric influence of the solar proton events and ground level enhancement in January 2005. Atmospheric Chemistry and Physics, 2011, 11, 6153-6166.	4.9	71
81	Composition changes after the "Halloween" solar proton event: the High Energy Particle Precipitation in the Atmosphere (HEPPA) model versus MIPAS data intercomparison study. Atmospheric Chemistry and Physics, 2011, 11, 9089-9139.	4.9	145
82	Modeling the atmospheric limb emission of CO2 at 4.3 μm in the terrestrial planets. Planetary and Space Science, 2011, 59, 988-998.	1.7	20
83	Non-LTE CO limb emission at in the upper atmosphere of Venus, Mars and Earth: Observations and modeling. Planetary and Space Science, 2011, 59, 1010-1018.	1.7	14
84	Analysis of Titan CH4 3.3μm upper atmospheric emission as measured by Cassini/VIMS. Icarus, 2011, 214, 571-583.	2.5	22
85	Distribution of HCN in Titan's upper atmosphere from Cassini/VIMS observations at 3μm. Icarus, 2011, 214, 584-595.	2.5	30
86	The science of EChO. Proceedings of the International Astronomical Union, 2010, 6, 359-370.	0.0	5
87	Do vibrationally excited OH molecules affect middle and upper atmospheric chemistry?. Atmospheric Chemistry and Physics, 2010, 10, 9953-9964.	4.9	9
88	Observations of infrared radiative cooling in the thermosphere on daily to multiyear timescales from the TIMED/SABER instrument. Journal of Geophysical Research, 2010, 115, .	3.3	102
89	Evidence for dynamical coupling from the lower atmosphere to the thermosphere during a major stratospheric warming. Geophysical Research Letters, 2010, 37, .	4.0	80
90	The Impact of Energetic Particle Precipitation on the Earths Atmosphere. Thirty Years of Astronomical Discovery With UKIRT, 2010, , 181-189.	0.3	1

#	Article	IF	CITATIONS
91	Kinetic temperature and carbon dioxide from broadband infrared limb emission measurements taken from the TIMED/SABER instrument. Advances in Space Research, 2009, 43, 15-27.	2.6	53
92	Influence of solar-geomagnetic disturbances on SABER measurements of 4.3μm emission and the retrieval of kinetic temperature and carbon dioxide. Advances in Space Research, 2009, 43, 1325-1336.	2.6	12
93	SABER observations of mesospheric ozone during NH late winter 2002–2009. Geophysical Research Letters, 2009, 36, .	4.0	57
94	Measurements of polar mesospheric clouds in infrared emission by MIPAS/ENVISAT. Journal of Geophysical Research, 2009, 114, .	3.3	15
95	Validation of Thermosphere Ionosphere Mesosphere Energetics and Dynamics/Sounding of the Atmosphere using Broadband Emission Radiometry (TIMED/SABER) v1.07 ozone at 9.6 <i>μ</i> m in altitude range 15–70 km. Journal of Geophysical Research, 2009, 114, .	3.3	45
96	Daytime SABER/TIMED observations of water vapor in the mesosphere: retrieval approach and first results. Atmospheric Chemistry and Physics, 2009, 9, 8139-8158.	4.9	23
97	Carbon monoxide distributions from the upper troposphere to the mesosphere inferred from 4.7 μm non-local thermal equilibrium emissions measured by MIPAS on Envisat. Atmospheric Chemistry and Physics, 2009, 9, 2387-2411.	4.9	77
98	Chemical heating rates derived from SCIAMACHY vibrationally excited OH limb emission spectra. Advances in Space Research, 2008, 41, 1914-1920.	2.6	20
99	About the increase of HNO ₃ in the stratopause region during the Halloween 2003 solar proton event. Geophysical Research Letters, 2008, 35, .	4.0	39
100	Assessment of the quality of the Version 1.07 temperatureâ€versusâ€pressure profiles of the middle atmosphere from TIMED/SABER. Journal of Geophysical Research, 2008, 113, .	3.3	369
101	Errors in Sounding of the Atmosphere using Broadband Emission Radiometry (SABER) kinetic temperature caused by nonâ€localâ€thermodynamicâ€equilibrium model parameters. Journal of Geophysical Research, 2008, 113, .	3.3	99
102	Enhancement of N ₂ O during the October–November 2003 solar proton events. Atmospheric Chemistry and Physics, 2008, 8, 3805-3815.	4.9	23
103	Model simulations of stratospheric ozone loss caused by enhanced mesospheric NO _x during Arctic Winter 2003/2004. Atmospheric Chemistry and Physics, 2008, 8, 5279-5293.	4.9	33
104	Validation of NO ₂ and NO from the Atmospheric Chemistry Experiment (ACE). Atmospheric Chemistry and Physics, 2008, 8, 5801-5841.	4.9	64
105	Short- and medium-term atmospheric constituent effects of very large solar proton events. Atmospheric Chemistry and Physics, 2008, 8, 765-785.	4.9	156
106	Ozone profile retrieval from limb scatter measurements in the HARTLEY bands: further retrieval details and profile comparisons. Atmospheric Chemistry and Physics, 2008, 8, 2509-2517.	4.9	6
107	Mesospheric N ₂ O enhancements as observed by MIPAS on Envisat during the polar winters in 2002–2004. Atmospheric Chemistry and Physics, 2008, 8, 5787-5800.	4.9	26
108	MIPAS: an instrument for atmospheric and climate research. Atmospheric Chemistry and Physics, 2008, 8, 2151-2188.	4.9	596

#	Article	IF	CITATIONS
109	CO measurements from the ACE-FTS satellite instrument: data analysis and validation using ground-based, airborne and spaceborne observations. Atmospheric Chemistry and Physics, 2008, 8, 2569-2594.	4.9	107
110	Global distribution of mean age of stratospheric air from MIPAS SF ₆ measurements. Atmospheric Chemistry and Physics, 2008, 8, 677-695.	4.9	105
111	Validation of MIPAS-ENVISAT NO ₂ operational data. Atmospheric Chemistry and Physics, 2007, 7, 3261-3284.	4.9	57
112	Validation of nitric acid retrieved by the IMK-IAA processor from MIPAS/ENVISAT measurements. Atmospheric Chemistry and Physics, 2007, 7, 721-738.	4.9	31
113	Key role of spin–orbit effects in the relaxation of CO2(010) by thermal collisions with O(3Pj). Molecular Physics, 2007, 105, 1171-1181.	1.7	11
114	Comment on "Origin of the January–April 2004 increase in stratospheric NO2observed in northern polar latitudes―by Jean-Baptiste Renard et al Geophysical Research Letters, 2007, 34, .	4.0	22
115	Fast forward radiative transfer modeling of 4.3μm nonlocal thermodynamic equilibrium effects for infrared temperature sounders. Geophysical Research Letters, 2007, 34, .	4.0	26
116	Evidence for N2Oν34.5μm non-local thermodynamic equilibrium emission in the atmosphere. Geophysical Research Letters, 2007, 34, .	4.0	5
117	Comparison of nighttime nitric oxide 5.3 <i>μ </i> m emissions in the thermosphere measured by MIPAS and SABER. Journal of Geophysical Research, 2007, 112, .	3.3	17
118	Ozone loss driven by nitrogen oxides and triggered by stratospheric warmings can outweigh the effect of halogens. Journal of Geophysical Research, 2007, 112, .	3.3	38
119	Global distributions of HO2NO2as observed by the Michelson Interferometer for Passive Atmospheric Sounding (MIPAS). Journal of Geophysical Research, 2007, 112, .	3.3	16
120	Analysis of nonlocal thermodynamic equilibrium CO 4.7μm fundamental, isotopic, and hot band emissions measured by the Michelson Interferometer for Passive Atmospheric Sounding on Envisat. Journal of Geophysical Research, 2007, 112, .	3.3	23
121	Ground-based mesospheric temperatures at mid-latitude derived from O2 and OH airglow SATI data: Comparison with SABER measurements. Journal of Atmospheric and Solar-Terrestrial Physics, 2007, 69, 2379-2390.	1.6	33
122	Satellite Measurements of Middle Atmospheric Impacts by Solar Proton Events in Solar Cycle 23. Space Science Reviews, 2007, 125, 381-391.	8.1	21
123	The Stratospheric and Mesospheric NOy in the 2002–2004 Polar Winters as measured by MIPAS/ENVISAT. Space Science Reviews, 2007, 125, 403-416.	8.1	29
124	Retrieval of stratospheric ozone profiles from MIPAS/ENVISAT limb emission spectra: a sensitivity study. Atmospheric Chemistry and Physics, 2006, 6, 2767-2781.	4.9	49
125	MIPAS level 2 operational analysis. Atmospheric Chemistry and Physics, 2006, 6, 5605-5630.	4.9	174

126 Global measurements and modeling of 4.3 um NLTE using AIRS. , 2006, 6362, 132.

0

#	Article	IF	CITATIONS
127	NO+ fundamental and first hot ro-vibrational line frequencies from MIPAS/Envisat atmospheric spectra. Journal of Molecular Spectroscopy, 2006, 237, 218-224.	1.2	7
128	Vibrationally excited ozone in the middle atmosphere. Journal of Atmospheric and Solar-Terrestrial Physics, 2006, 68, 202-212.	1.6	26
129	Vibrational quenching of CO2(010) by collisions with O(P3) at thermal energies: A quantum-mechanical study. Journal of Chemical Physics, 2006, 124, 164302.	3.0	15
130	Remote Sensing of the Non-LTE Atmosphere. , 2006, , 87-106.		1
131	Comparisons of MIPAS/ENVISAT and GPS-RO/CHAMP Temperatures. , 2005, , 567-572.		1
132	Comparison of GPS/SAC-C and MIPAS/ENVISAT Temperature Profiles and Its Possible Implementation for EOS MLS Observations. , 2005, , 573-578.		3
133	A comparison of night-time GOMOS and MIPAS ozone profiles in the stratosphere and mesosphere. Advances in Space Research, 2005, 36, 958-966.	2.6	22
134	Meteorological results from the Global Mars Multiscale Model at the Viking 1 lander site. Advances in Space Research, 2005, 36, 2169-2175.	2.6	4
135	Analysis of non-LTE emissions at in the Martian atmosphere as observed by PFS/Mars Express and SWS/ISO. Planetary and Space Science, 2005, 53, 1079-1087.	1.7	35
136	Retrieval of stratospheric and mesospheric O3 from high resolution MIPAS spectra at 15 and 10 μm. Advances in Space Research, 2005, 36, 943-951.	2.6	21
137	Atmospheric non-local thermodynamic equilibrium emissions as observed by the Michelson Interferometer for Passive Atmospheric Sounding (MIPAS). Comptes Rendus Physique, 2005, 6, 848-863.	0.9	20
138	Comparisons of MIPAS/ENVISAT ozone profiles with SMR/ODIN and HALOE/UARS observations. Advances in Space Research, 2005, 36, 927-931.	2.6	9
139	Cross comparisons of O3 and NO2 measured by the atmospheric ENVISAT instruments GOMOS, MIPAS, and SCIAMACHY. Advances in Space Research, 2005, 36, 855-867.	2.6	34
140	Evidence for CH47.6 μm non-local thermodynamic equilibrium emission in the mesosphere. Geophysical Research Letters, 2005, 32, n/a-n/a.	4.0	8
141	Rotational and spin-orbit distributions of NO observed by MIPAS/ENVISAT during the solar storm of October/November 2003. Journal of Geophysical Research, 2005, 110, .	3.3	23
142	Retrieval of stratospheric NOxfrom 5.3 and 6.2 μm nonlocal thermodynamic equilibrium emissions measured by Michelson Interferometer for Passive Atmospheric Sounding (MIPAS) on Envisat. Journal of Geophysical Research, 2005, 110, .	3.3	84
143	NOyfrom Michelson Interferometer for Passive Atmospheric Sounding on Environmental Satellite during the Southern Hemisphere polar vortex split in September/October 2002. Journal of Geophysical Research, 2005, 110, .	3.3	32
144	Validation of stratospheric temperatures measured by Michelson Interferometer for Passive Atmospheric Sounding (MIPAS) on Envisat. Journal of Geophysical Research, 2005, 110, .	3.3	16

#	Article	IF	CITATIONS
145	Longitudinal variations of temperature and ozone profiles observed by MIPAS during the Antarctic stratosphere sudden warming of 2002. Journal of Geophysical Research, 2005, 110, .	3.3	9
146	Observation of NOxenhancement and ozone depletion in the Northern and Southern Hemispheres after the October-November 2003 solar proton events. Journal of Geophysical Research, 2005, 110, .	3.3	132
147	HNO3, N2O5, and ClONO2enhancements after the October-November 2003 solar proton events. Journal of Geophysical Research, 2005, 110, .	3.3	69
148	Experimental evidence of perturbed odd hydrogen and chlorine chemistry after the October 2003 solar proton events. Journal of Geophysical Research, 2005, 110, .	3.3	55
149	Energy transport in the thermosphere during the solar storms of April 2002. Journal of Geophysical Research, 2005, 110, .	3.3	105
150	Water vapor distributions measured with the Michelson Interferometer for Passive Atmospheric Sounding on board Envisat (MIPAS/Envisat). Journal of Geophysical Research, 2005, 110, .	3.3	63
151	An enhanced HNO3second maximum in the Antarctic midwinter upper stratosphere 2003. Journal of Geophysical Research, 2005, 110, .	3.3	52
152	Downward transport of upper atmospheric NOxinto the polar stratosphere and lower mesosphere during the Antarctic 2003 and Arctic 2002/2003 winters. Journal of Geophysical Research, 2005, 110, .	3.3	131
153	Thermospheric infrared radiance response to the April 2002 geomagnetic storm from SABER infrared and GUVI ultraviolet limb data. , 2004, , .		6
154	SABER observations of mesospheric temperatures and comparisons with falling sphere measurements taken during the 2002 summer MaCWAVE campaign. Geophysical Research Letters, 2004, 31, .	4.0	174
155	Evidence for an OH(ï) excitation mechanism of CO24.3 μm nighttime emission from SABER/TIMED measurements. Journal of Geophysical Research, 2004, 109, .	3.3	31
156	Cross-validation of MIPAS/ENVISAT and GPS-RO/CHAMP temperature profiles. Journal of Geophysical Research, 2004, 109, .	3.3	27
157	Comparisons of MIPAS-observed temperature profiles with other satellite measurements. , 2004, , .		5
158	Modelling of atmospheric mid-infrared radiative transfer: the AMIL2DA algorithm intercomparison experiment. Journal of Quantitative Spectroscopy and Radiative Transfer, 2003, 78, 381-407.	2.3	45
159	The natural thermostat of nitric oxide emission at 5.3 μm in the thermosphere observed during the solar storms of April 2002. Geophysical Research Letters, 2003, 30, .	4.0	123
160	A blind test retrieval experiment for infrared limb emission spectrometry. Journal of Geophysical Research, 2003, 108, .	3.3	57
161	Retrieval of kinetic temperature and carbon dioxide abundance from nonlocal thermodynamic equilibrium limb emission measurements made by the SABER experiment on the TIMED satellite. , 2003, , .		16

Remote sensing of the middle atmosphere with MIPAS. , 2003, , .

#	Article	IF	CITATIONS
163	Validation of MIPAS/ENVISAT level-1B data products. , 2003, , .		1
164	Early IMK/IAA MIPAS/ENVISAT results. , 2003, 4882, 184.		7
165	Non-LTE studies for the analysis of MIPAS/ENVISAT data. , 2002, , .		2
166	New non-LTE retrieval method for atmospheric parameters from MIPAS/ENVISAT emission spectra at 5.3 μ m. , 2002, 4539, 396.		2
167	Intercomparison of radiative transfer codes under non-local thermodynamic equilibrium conditions. Journal of Geophysical Research, 2002, 107, ACH 12-1.	3.3	22
168	Impact of non-LTE processes on middle atmospheric water vapor retrievals from simulated measurements of 6.8 μm Earth limb emission. Geophysical Research Letters, 2002, 29, 2-1-2-4.	4.0	7
169	Retrieval of mesospheric and lower thermospheric kinetic temperature from measurements of CO215 µm Earth Limb Emission under non-LTE conditions. Geophysical Research Letters, 2001, 28, 1391-1394.	4.0	241
170	Latitudinal and longitudinal behavior of the mesospheric OH nightglow layer as observed by the Improved Stratospheric and Mesospheric Sounder on UARS. Journal of Geophysical Research, 2001, 106, 8027-8033.	3.3	12
171	A new non-LTE retrieval method for atmospheric parameters from mipas-envisat emission spectra. Advances in Space Research, 2001, 27, 1099-1104.	2.6	49
172	Non-LTE Radiative Mesospheric Study for Mars Pathfinder Entry. Icarus, 2000, 146, 360-365.	2.5	9
173	Non-LTE Infrared Emissions of CO2 in the Atmosphere of Venus. Icarus, 2000, 147, 11-25.	2.5	45
174	Non-LTE state distribution of nitric oxide and its impact on the retrieval of the stratospheric daytime no profile from MIPAS limb sounding instruments. Advances in Space Research, 2000, 26, 947-950.	2.6	8
175	A review of CO2 and CO abundances in the middle atmosphere. Geophysical Monograph Series, 2000, , 83-100.	0.1	41
176	Optimized spectral microwindows for data analysis of the Michelson Interferometer for Passive Atmospheric Sounding on the Environmental Satellite. Applied Optics, 2000, 39, 5531.	2.1	45
177	Global distribution of CO2in the upper mesosphere as derived from UARS/ISAMS measurements. Journal of Geophysical Research, 2000, 105, 19829-19839.	3.3	15
178	Evidence of H2O nonlocal thermodynamic equilibrium emission near 6.4 μm as measured by cryogenic infrared spectrometers and telescopes for the atmosphere (CRISTA 1). Journal of Geophysical Research, 2000, 105, 29003-29021.	3.3	8
179	Antarctic polar descent and planetary wave activity observed in ISAMS CO from April to July 1992. Geophysical Research Letters, 2000, 27, 665-668.	4.0	36

Nonlocal thermodynamic equilibrium vibrational, rotational, and spin state distribution of NO($\hat{1}_{2}^{\prime}=0, 1$,) Tj ETQq0 0.0 rgBT /Qverlock 10

#	Article	IF	CITATIONS
181	Kinetic requirements for the measurement of mesospheric water vapor at 6.8 µm under non-LTE conditions. Geophysical Research Letters, 1999, 26, 63-66.	4.0	11
182	Evidence of non-LTE effects in mesospheric water vapor from spectrally-resolved emissions observed by CIRRIS-1A. Geophysical Research Letters, 1999, 26, 67-70.	4.0	13
183	Correlation between ISAMS and ATMOS measurements of co in the middle atmosphere. Advances in Space Research, 1998, 22, 1517-1520.	2.6	2
184	Evidences of non-LTE emission in the ISAMS water vapour channels. Advances in Space Research, 1998, 22, 1513-1516.	2.6	1
185	Modelling of non-LTE limb spectra of i.r. ozone bands for the MIPAS space experiment. Journal of Quantitative Spectroscopy and Radiative Transfer, 1998, 59, 405-422.	2.3	28
186	The non-LTE correction to the vibrational component of the internal partition sum for atmospheric calculations. Journal of Quantitative Spectroscopy and Radiative Transfer, 1998, 59, 423-436.	2.3	19
187	Non-local thermodynamic equilibrium limb radiances for the mipas instrument on Envisat-1. Journal of Quantitative Spectroscopy and Radiative Transfer, 1998, 59, 377-403.	2.3	17
188	Modelling of the non-LTE populations of thenitricacid and methane vibrational states in themiddleatmosphere. Journal of Atmospheric and Solar-Terrestrial Physics, 1998, 60, 1631-1647.	1.6	9
189	The detection of the hydroxyl nightglow layer in the mesosphere by ISAMS/UARS. Geophysical Research Letters, 1998, 25, 2417-2420.	4.0	4
190	Non local thermodynamic equilibrium (LTE) atmospheric limb emission at 4.6 μm: 2. An analysis of the daytime wideband radiances as measured by UARS improved stratospheric and mesospheric sounder. Journal of Geophysical Research, 1998, 103, 8515-8530.	3.3	23
191	Non local thermodynamic equilibrium (LTE) atmospheric limb emission at 4.6 μm: 1. An update of the CO2non-LTE radiative transfer model. Journal of Geophysical Research, 1998, 103, 8499-8513.	3.3	32
192	Non-local thermodynamic equilibrium in H2O 6.9 \hat{l} /4m emission as measured by the improved stratospheric and mesospheric sounder. Journal of Geophysical Research, 1998, 103, 31293-31308.	3.3	11
193	Non-local thermodynamic equilibrium in general circulation models of the Martian atmosphere 1. Effects of the local thermodynamic equilibrium approximation on thermal cooling and solar heating. Journal of Geophysical Research, 1998, 103, 16799-16811.	3.3	52
194	Upper mesosphere temperatures in summer: WINDII observations and comparisons. Geophysical Research Letters, 1997, 24, 357-360.	4.0	18
195	Evidence of non-LTE in the CO215µm weak bands from ISAMS and WINDII observations. Geophysical Research Letters, 1997, 24, 361-364.	4.0	7
196	Validation of measurements of carbon monoxide from the improved stratospheric and mesospheric sounder. Journal of Geophysical Research, 1996, 101, 9929-9955.	3.3	39
197	Measurements of water vapor distributions by the improved stratospheric and mesospheric sounder: Retrieval and validation. Journal of Geophysical Research, 1996, 101, 9907-9928.	3.3	20
198	Non-local thermodynamic equilibrium limb radiance near 10 μm as measured by UARS CLAES. Journal of Geophysical Research, 1996, 101, 26577-26588.	3.3	22

#	Article	IF	CITATIONS
199	<title>Retrieval of pressure and temperature from MIPAS-ENVISAT limb emission spectra</title> . , 1996, ,		0
200	Radiative Energy Balance of CO2 Non-LTE Infrared Emissions in the Martian Atmosphere. Icarus, 1995, 114, 113-129.	2.5	34
201	Non-local thermodynamic equilibrium model for H2O 6.3 and 2.7-μm bands in the middle atmosphere. Journal of Geophysical Research, 1995, 100, 9131.	3.3	35
202	Rapid computation of spectrally integrated non-LTE limb emission. , 1994, 2266, 425.		2
203	Stratospheric and mesospheric carbon monoxide. First results from the validation of the isams measurements at 4.6 μm. Advances in Space Research, 1994, 14, 233-236.	2.6	1
204	Non-local thermodynamic equilibrium limb radiance from O3 and CO2 in the 9–11 μm spectral region. Journal of Quantitative Spectroscopy and Radiative Transfer, 1994, 52, 389-407.	2.3	16
205	Comparison of line-by-line and curtis matrix calculations for the vibrational temperatures and radiative cooling of the CO2 15 μm bands in the middle and upper atmosphere. Journal of Quantitative Spectroscopy and Radiative Transfer, 1994, 52, 409-423.	2.3	6
206	Rapid computation of spectrally integrated non-local thermodynamic equilibrium limb emission. Journal of Geophysical Research, 1994, 99, 25761.	3.3	16
207	A non-local thermodynamic equilibrium radiative transfer model for infrared emissions in the atmosphere of Mars: 1. Theoretical basis and nighttime populations of vibrational levels. Journal of Geophysical Research, 1994, 99, 13093.	3.3	39
208	A non-local thermodynamic equilibrium radiative transfer model for infrared emissions in the atmosphere of Mars: 2. Daytime populations of vibrational levels. Journal of Geophysical Research, 1994, 99, 13117.	3.3	28
209	Global and seasonal variations in middle atmosphere CO from UARS/ISAMS. Geophysical Research Letters, 1993, 20, 1247-1250.	4.0	18
210	Nonâ€localâ€thermodynamicâ€equilibrium populations of the first vibrational excited state of CO in the middle atmosphere. Journal of Geophysical Research, 1993, 98, 8933-8947.	3.3	19
211	Nonâ€local thermodynamic equilibrium studies of the 15â€Î¼m bands of CO ₂ for atmospheric remote sensing. Journal of Geophysical Research, 1993, 98, 14955-14977.	3.3	60
212	Local thermodynamic equilibrium of carbon dioxide in the upper atmosphere. Geophysical Research Letters, 1992, 19, 589-592.	4.0	49
213	Analysis of the upper atmosphere CO ₂ (<i>v</i> ₂) vibrational temperatures retrieved from ATMOS/Spacelab 3 observations. Journal of Geophysical Research, 1992, 97, 20469-20478.	3.3	55
214	Vibrational temperatures and radiative cooling of the CO ₂ 15 <i>μ</i> m bands in the middle atmosphere. Quarterly Journal of the Royal Meteorological Society, 1992, 118, 499-532.	2.7	25
215	Studies of Solar Heating by CO2in the Upper Atmosphere Using a Non-LTE Model and Satellite Data. Journals of the Atmospheric Sciences, 1990, 47, 809-822.	1.7	22
216	Carbon dioxide 4.3â€Î¼m emission in the Earth's atmosphere: A comparison between Nimbus 7 SAMS measurements and nonâ€local thermodynamic equilibrium radiative transfer calculations. Journal of Geophysical Research, 1989, 94, 13045-13068.	3.3	39

#	Article	IF	CITATIONS
217	Rocket measurements of O2 infrared atmospheric system in the nightglow. Planetary and Space Science, 1988, 36, 459-467.	1.7	19
218	Altitude distribution of vibrationally excited states of atmospheric hydroxyl at levels v = 2 to v = 7. Planetary and Space Science, 1987, 35, 1029-1038.	1.7	71
219	Neutral atmospheric composition between 60 and 220 km: A theoretical model for mid-latitudes. Planetary and Space Science, 1986, 34, 723-743.	1.7	62
220	A non-LTE radiative transfer model for infrared bands in the middle atmosphere. I. Theoretical basis and application to CO2 15 μm bands. Journal of Atmospheric and Solar-Terrestrial Physics, 1986, 48, 729-748.	0.9	80
221	A non-LTE radiative transfer model for infrared bands in the middle atmosphere. II. CO2 (2.7 and 4.3 μm) and water vapour (6.3 μm) bands and N2(1) and O2(1) vibrational levels. Journal of Atmospheric and Solar-Terrestrial Physics, 1986, 48, 749-764.	0.9	60
222	Gravity waves from five simultaneous emissions: OH (6–2), NaD, O ₂ (¹ Σ), Ol–557.7â€,nm, and the visible continuum. Canadian Journal of Physics, 1985, 63, 592-599.	1.1	7
223	Analysis of OI-557.7 nm, NaD, OH(6-2) and nightglow emissions from ground-based observations. Journal of Atmospheric and Solar-Terrestrial Physics, 1985, 47, 1099-1110.	0.9	19
224	Moderately misaligned orbit of the warm sub-Saturn HD332231 b. Astronomy and Astrophysics, 0, , .	5.1	5
225	The CH4 abundance in Jupiter's upper atmosphere. Astronomy and Astrophysics, 0, , .	5.1	2